# Interaction between RNF8 and DYRK2 is required for the recruitment of DNA repair molecules to DNA double-strand breaks

Takenori Yamamoto[1,‡], Naoe Taira Nihira[1,†,‡], Satomi Yogosawa[1], Katsuhiko Aoki[1], Hiroyuki Takeda[2], Tatsuya Sawasaki[2] and Kiyotsugu Yoshida[1]

1 Department of Biochemistry, Jikei University School of Medicine, Minato-ku, Tokyo, Japan
2 Cell-Free Science and Technology Research Center, Ehime University, Matsuyama, Ehime, Japan

**Correspondence**
K. Yoshida, Department of Biochemistry, Jikei University Schools of Medicine, 3-25-8 Nishi-shinbashi, Minato-ku, Tokyo 105-8461, Japan
Fax: +81 3 3435 1922
Tel: +81 3 3433 1111
E-mail: kyoshida@jikei.ac.jp

**†Present address**
Department of Pathology, Beth Israel Deaconess Medical Center, Harvard Medical School, Boston, MA, 02215, USA

‡These authors contributed equally to this work

The genome of eukaryotic cells is frequently exposed to damage by various genotoxins. Phosphorylation of histone H2AX at Serine 139 (γ-H2AX) is a hallmark of DNA damage. RNF8 monoubiquitinates γ-H2AX with the Lys63-linked ubiquitin chain to tether DNA repair molecules at DNA lesions. A high-throughput screening identified RNF8 as a binding partner of dual-specificity tyrosine phosphorylation-regulated kinase 2 (DYRK2). Notably, DNA damage-induced monoubiquitination of γ-H2AX is impaired in DYRK2-depleted cells. The foci formation of p53-binding protein 1 at DNA double-strand break sites is suppressed in DYRK2 knockdown cells, which fail to repair the DNA damage. A homologous recombination assay showed decreased repair efficiency in DYRK2-depleted cells. Our findings indicate direct interaction of DYRK2 with RNF8 in regulating response to DNA damage.

**Keywords:** DNA damage; DNA repair; DYRK2; RNF8; γH2AX monoubiquitination

Cells have the ability to sense and repair DNA lesions caused by DNA damage and DNA replication stress. For sensing DNA damage, post-translational modifications, particularly ubiquitination and phosphorylation, are involved in a central regulatory mechanism. Ataxia telangiectasia-mutated (ATM) and Rad3-related (ATR) protein kinases are involved in the recognition of DNA winding and DNA lesions. In response to DNA double-strand breaks (DSBs), ATM is activated by its autophosphorylation. Activated ATM phosphorylates histone H2AX, breast cancer 1 (BRCA1), checkpoint kinase (Chk) 2, and Nibrin or Nijmegen breakage syndrome 1 (Nbs1) proteins to repair the damaged DNA [1]. Histone H2AX is one of the most conserved variants of Histone H2A having extra amino acid sequences in the C terminus compared to Histone H2A. ATM-mediated Histone H2AX phosphorylation at Ser139 (γ-H2AX) is a hallmark of DSB sites [2]. Mediator of DNA damage checkpoint protein 1 (MDC1) binds to phosphorylated γ-H2AX. Additionally this, phosphorylation promotes the binding of RNF8 (an E3 ubiquitin ligase) with MDC1 on DNA

lesions. RNF8 contains an N-terminal forkhead-associated (FHA) domain and a C-terminal RING-finger domain responsible for its ubiquitin ligase activity [3]. FHA domains recognize exclusively phospho-threonine (pThr)-containing motifs, compared to BRCA1 carboxyl terminus (BRCT) domains that recognize both phospho-serine- (pSer) and pThr-containing sequences. Accordingly, RNF8 specifically binds to Thr-phosphorylated substrates [4]. RNF8 recognizes three pTQXF motifs in MDC1 [5]. Together with the E2-conjugating enzyme UBC13, RNF8 catalyzes histone H2AX Lys 63-linked ubiquitination in response to DSBs. Ubiquitinated histone H2AX tethers DNA repair factors including RNF8, p53-binding protein 1 (53BP1), and BRCA1 to the DSB sites, thereby initiating homologous recombination (HR) [6].

Dual-specificity tyrosine phosphorylation-regulated kinase 2 (DYRK2) is a Ser/Thr kinase that regulates cell cycle progression, cell migration, and apoptosis. DYRK2-depleted cancer cells exhibit aberrant cell growth and metastasis [7,8]. Immunohistochemical analysis indicated significant reduction in DYRK2 expression in invasive breast tumor tissues. Resistance of ovarian cancer cells to cisplatin is associated with reduced DYRK2 expression, indicating its tumor-suppressive role [9]. In response to genotoxic stress, DYRK2 phosphorylates p53 at Ser46 [10]. Ser46 phosphorylation is detected in the later stages of genotoxic stimuli-induced signaling, and it contributes to the induction of cell death [11,12]. In a genome-wide shRNA screening aimed at identifying the molecules involved in DNA repair, DYRK2 was ranked among the top 38 candidates [13]. However, it remains unclear whether DYRK2 physiologically affects DNA repair.

Here, we demonstrated that DYRK2 regulated the ubiquitination activity of RNF8 through direct interaction. Depletion of DYRK2 impaired 53BP1 foci formation at DSB sites, and down-regulated the repair efficiency, resulting in unsuccessful repair of DNA lesions.

## Materials and methods

### Screening for E3 ubiquitin ligases that interact with DYRK2

E3 ligase screening and cell-free synthesized E3 ubiquitin ligase protein array used in the present study were as described previously [14]. Briefly, FLAG-DYRK2 and FLAG-dihydrofolate reductase (DHFR) were synthesized using wheat cell-free protein synthesis system [15,16]. E3 ligase protein array containing 223 N-terminal biotinylated E3 ligases was established using the mammalian gene collection (MGC) cDNA clone set [17] and functional annotation

of mouse (FANTOM) cDNA clone set [18]. Biotinylated E3 ligases were synthesized using wheat germ cell-free synthesis system. Biotinylation of the biotin ligation site was accomplished using enzymatic biotinylation with BirA biotin ligase [19] and biotin (Sigma, St. Louis, MO, USA). All AlphaScreen reactions were conducted in an Optiplate 384 titer plate (PerkinElmer, Waltham, MA, USA). One microliter of cell-free synthesized FLAG-tagged bait protein and 1 μL of biotinylated prey protein were mixed in 15 μL of AlphaScreen buffer containing 100 mM Tris-HCl (pH8.0), 0.01% Tween 20, 100 mM NaCl, and 1 mg·mL$^{-1}$ BSA. Dispensing and mixing of proteins in a 384-well plate were carried out using Janus automated liquid handling workstation (PerkinElmer). The mixture was incubated at 26 °C for 30 min. Subsequently, 10 μL of detection mixture containing 0.025 μL of anti-FLAG M2 antibody (Sigma), 0.1 μL of streptavidin-conjugated AlphaScreen donor beads, and 0.1 μL of protein A-conjugated AlphaScreen acceptor beads in AlphaScreen buffer was added to the mixture using FlexDrop dropper (PerkinElmer). After incubation at 26 °C for 1 h, AlphaScreen chemiluminescence signal was detected using EnVision multilabel plate reader (PerkinElmer).

### Cell culture and treatment

Cells of the human osteosarcoma cell line U2OS were cultured in Roswell Park Memorial Institute (RPMI) 1640 media supplemented with 10% heat-inactivated FBS, 100 U·mL$^{-1}$ penicillin, 100 μg·mL$^{-1}$ streptomycin, and 2 mM L-glutamine at 37 °C in 5% $CO_2$. Human embryonic kidney 293T cells were grown in Dulbecco's modified Eagle medium (DMEM) containing 10% heat-inactivated FBS, 100 U·mL$^{-1}$ penicillin, 100 μg·mL$^{-1}$ streptomycin, and 2 mM L-glutamine at 37 °C in 5% $CO_2$. U2OS cells were treated with 2 μg·mL$^{-1}$ Adriamycin (ADR) for 0.5, 1, 2, 4, 6, 8, and 24 h (Sigma-Aldrich) or 5 μM Harmine for 0.5 and 1 h (Abcam) at 37 °C in 5% $CO_2$.

### Plasmids

Flag-tagged DYRK2 and GFP-tagged DYRK2$^{K178R}$ mutant were cloned as previously described [10]. RNF8 cDNA was amplified by PCR and cloned into the pEGFP-C1 vector. Site-directed mutagenesis was performed using PCR and verified by DNA sequencing. The GFP-tagged RNF8$^{C403S}$ mutant plasmid (gifted by S. Nakada, Osaka University) was cloned into the mCherry vector.

### Cell Transfection

The RNF8-specific siRNA, DYRK2-specific siRNA, and control siRNA were purchased from Qiagen, Sigma, and Invitrogen, respectively. Transfections of validated gene-specific siRNAs were performed using Lipofectamine RNAi MAX (Invitrogen, Carlsbad, CA, USA) according to the

supplied protocol. Flag-tagged DYRK2 and GFP-tagged RNF8 plasmids were transfected using FuGENE HD. The GFP-tagged DYRK2$^{K178R}$ mutant and the mCherry-tagged RNF8$^{C403S}$ mutant were transfected using X-tremeGENE9 (Roche, Basel, Switzerland) following the manufacturer's protocol.

## Immunoprecipitation

293T cells were harvested, washed in phosphate-buffed saline (PBS), and resuspended in lysis buffer (50 mM Tris-HCl, pH 7.6, 150 mM NaCl, 10 mM NaF, 1 mM Na$_3$VO$_4$, 1 mM PMSF, 1 mM DTT, 10 μg·mL$^{-1}$ aprotinin, 1 μg·mL$^{-1}$ leupeptin, 1 μg·mL$^{-1}$ pepstatin A, and 1% NP-40). After centrifugation, supernatants were isolated and used as cell lysates. For immunoprecipitation, lysates were incubated with anti-Flag-agarose (Sigma-Aldrich) for 2 h at 4 °C. The immunoprecipitates were washed three times with lysis buffer. The bound proteins were eluted with SDS sample buffer and boiled for 5 min.

## Immunoblotting

293T cells and U2OS cells were washed with PBS three times and then incubated with 10% trichloroacetic acid for 5 min. Cells were lifted and suspended in SDS sample buffer. Lysates were sonicated on ice. Cell extracts were separated by SDS/ PAGE and transferred on nitrocellulose membranes. The membranes were probed with anti-γH2AX (Millipore, Darmstadt, Germany), anti-H2AX (Cell Signaling Technology, Washington, DC, USA), anti-DYRK2 (Human Protein Atlas, Bromma, Sweden), anti-RNF8 (Santa Cruz Biotechnology, Dallas, TX, USA), anti-phospho-p53 (Ser46) (Bio Academia, Osaka, Japan), anti-p53 (Santa Cruz Biotechnology), anti-GST (Nacalai Tesque, Kyoto, Japan), anti-Tubulin (Sigma), anti-GAPDH (Chemicon, Darmstadt, Germany), anti-Flag (Cell Signaling Technology), or anti-GFP (Nacalai Tesque). Immune complexes were incubated with secondary antibodies and visualized using western lightning chemiluminescence reagent (PerkinElmer Life Sciences).

## *In vitro* kinase assay

Recombinant His-DYRK2 protein was obtained from Merck. Recombinant GST-p53 was used as a substrate from the previous study [10]. His-DYRK2 was incubated in the kinase buffer (20 mM HEPES; pH 7.0, 10 mM MgCl$_2$, 10 mM MnCl$_2$, 0.1 mM Na$_3$VO$_4$, and 2 mM dithiothreitol) with GST-p53 and/or Harmine along with ATP for 5 min at 30 °C. Reaction products were subjected to immunoblot analysis.

## Comet assay

The alkaline comet assay was performed as described by Benjamin *et al*. [20,21]. U2OS cells treated in the presence or absence of ADR or DYRK2 siRNA or Hydrogen peroxide (H$_2$O$_2$) were combined with molten LM Agarose (Trevigen, Gaithersburg, MD, USA) at 37 °C with a ratio of 1 : 10 (v/v), and immediately spread onto CometSlide (Trevigen). After 10 min of gelling at 4 °C, the cells were lysed with lysis solution (Trevigen) at 4 °C for 1 h. The slides were placed in a horizontal electrophoresis tank containing electrophoresis solution (200 mM NaOH, and 1 mM EDTA; pH > 13) and electrophoresis was ran for 30 min (21 V/cm). After electrophoresis, the slides were washed in distilled water for two times and immersed in 70% ethanol for 5 min and dried at 37 °C for 10–15 min, and then stained with SYBR Gold Staining solution for 30 min. After staining, the slides were washed in distilled water and dried at 37 °C for 30 min. Comet images were captured using a Zeiss Axioplan fluorescent microscope. The images were analyzed using OPENCOMET software and COMETSCORE version 1.5 software [20]. The extent of DNA damage was expressed as a measure of percentage of DNA in tail.

## Immunofluorescence assay

The U2OS cells were seeded and cultured in the presence or absence of ADR or irradiation (2 Gy). Cells were permeabilized using 0.5% Triton X-100 in PBS for 15 min at room temperature and fixed with formaldehyde in PBS for 20 min at 4 °C. After fixation, cells were washed with PBS and blocked with 2% BSA (bovine serum albumin) for 1 h. After washing, cells were incubated with anti-DYRK2 (Human Protein Atlas) or anti-53BP1 (BD Bioscience, Franklin Lakes, NJ, USA) or anti-γH2AX (Millipore) overnight at 4 °C. Immune complexes were incubated with FITC-conjugated secondary antibodies or/ and Alexa flour 594 goat anti-(mouse IgG) (Life technologies, Carlsbad, CA, USA) or Alexa flour 555 goat anti-(mouse IgG) (Cell Signaling Technology) for 1 h at room temperature. Nuclei were stained with DAPI (Vector Laboratories, Burlingame, CA, USA). Fixed cells were imaged at room temperature using an all-in-one type fluorescence microscope (Biozero-8000, Keyence, Osaka, Japan) equipped with a Plan Apochromat 20×/0.75 NA objective lens (Nikon, Tokyo, Japan) and confocal laser scanning microscope equipped with Airyscan (LSM-880, ZEISS). For live imaging, U2OS cells were seeded and cultured in the 3.5-cm dishes and then cotransfected with mCherry-tagged RNF8$^{C403S}$ mutant and GFP-tagged DYRK2$^{K178R}$ mutant. After irradiation (10 Gy), cells were observed by using a fluorescence microscope (Biozero-8000; Keyence) equipped with a Plan Apochromat 20 × /0.75 NA objective lens and (Nikon).

## DNA damage

U2OS cells were exposed to X-rays using a Model MBR-1520R-3 irradiator (HITACHI, Tokyo, Japan).

## Homologous recombination assay

U2OS cell carrying the DR (direct repeat)-GFP homologous recombination reporter was used for the analysis of HR. For analyses with siRNA, cells were transfected with control siRNA or DYRK2 siRNA and cultured in 6-cm dishes for 48 h. After the medium was changed, the cells were then transfected with 3.0 µg (DR-GFP assay) of pCBASceI (the I-SceI expression plasmid) using Xtreme-GENE9 (Roche). Cells were collected 48 h post plasmid transfection via trypsinization, washed twice with PBS, suspended in 0.1% FBS/PBS, and fixed with formaldehyde. The proportion of GFP-positive cells was determined using flow cytometry using a MACSQuant analyzer 10 (Miltenyi Biotec, Cologne, Germany).

## Cell cycle analysis

U2OS cells carrying the DR (direct repeat)-GFP homologous recombination reporter were washed with chilled PBS and resuspended with PBS. After washing, cells were fixed with 70% ethanol and incubated with RNase and 7-AAD (7-Aminoactinomycin D) for 30 min at 37 °C. Data from the flow cytometry were acquired and analyzed using a MACSQuant analyzer 10 (Miltenyi Biotec).

## Statistics

Statistical analysis was performed using Student's *t*-test. Data represent the mean ± SD.

$P < 0.05$ was considered as statistically significant.

# Results

## RNF8 is a novel-binding protein of DYRK2

Along with E3 ubiquitin ligases, DYRK2 promotes proteasome degradation of c-Jun, c-Myc, Snail, TERT, and Katanin p60 [22]. DYRK2 functions as a scaffold protein in the EDD-DDB1-VprBP (EDVP) E3 ligase complex associated with the degradation of TERT and Katanin p60 [23,24]. To further define the characteristics of DYRK2, we screened for DYRK2-interacting E3 ubiquitin ligase(s) using a protein array generated by the wheat germ cell-free protein synthesis system. The screening process identified, four E3 ubiquitin ligases as potential *in vitro* binding proteins of DYRK2 (Fig. 1A). Notably, in this screening, murine double minute 2 (MDM2) was screened out with the highest score. In our previous study, we demonstrated that DYRK2 is ubiquitinated by MDM2 under unstressed conditions [25], suggesting the identification of physiologically interacting proteins of DYRK2 by this screening process. Subsequently, we examined the interaction of DYRK2 with RNF8 in

cells, which was identified as one of the promising candidates in the screening process. To confirm the screening results, 293T cells were cotransfected with GFP-vector or GFP-tagged RNF8 and Flag-vector or Flag-tagged DYRK2 (Fig. 1B). Ectopically expressed RNF8 interacted with DYRK2 in 293T cells. However, we could not detect endogeneous interaction between DYRK2 and RNF8 due to an unavailability of antibodies immunoprecipitating endogeneous DYRK2 or RNF8. Given that RNF8 is an E3 ubiquitin ligase, we hypothesized that RNF8 down-regulated DYRK2 expression by ubiquitination. However, the expression of DYRK2 remained unchanged in RNF8 knockdown cells (Fig. 1C). These results demonstrated that RNF8 interacted with DYRK2 in the cells, but it was not involved in the degradation of DYRK2, indicating the possible regulation of RNF8 function by DYRK2.

## DYRK2 is essential for the monoubiquitination of γ-H2AX in response to genotoxic stress

Accumulating studies have shown the involvement of RNF8-mediated monoubiquitination of Histone H2A in the recruitment of DNA repair proteins at DSBs. In response to DNA damage, ATM protein kinase is activated and phosphorylates histone H2AX, a variant of histone H2A, at Ser139. ATM also phosphorylates MDC1. RNF8 binds to phosphorylated MDC1 and ubiquitinates ATM-phosphorylated H2AX (γ-H2AX) [26]. Ubiquitinated γ-H2AX promotes the recruitment of BRCA1 and 53BP1 at DSB sites. To evaluate the activity of RNF8 upon DNA damage, we monitored the level of endogenous γ-H2AX monoubiquitination in response to genotoxic stress (Fig. 2A). As expected, γ-H2AX was monoubiquitinated in the early phase after DNA damage. To examine the role of DYRK2 in the RNF8-mediated monoubiquitination of γ-H2AX, U2OS cells were transfected with control siRNA or DYRK2-specific siRNA followed by ADR treatment, which triggered DSBs (Fig. 2B). Monoubiquitination of γ-H2AX was observed after an hour of DNA damage in U2OS cells transfected with control siRNA. However, knocking down DYRK2 attenuated γ-H2AX monoubiquitination. Also, we confirmed that γ-H2AX monoubiquitination was not detected in the RNF8 knocking down cells (Fig. 2B). To exclude the possibility of association of knocking down DYRK2 with off-target effects, two DYRK2 siRNAs that target different sequences of DYRK2 were transfected into U2OS cells followed by ADR treatment (Fig. S1A). Both the siRNAs attenuated γ-H2AX monoubiquitination in response to DNA damage,

**A**



**B**



**C**
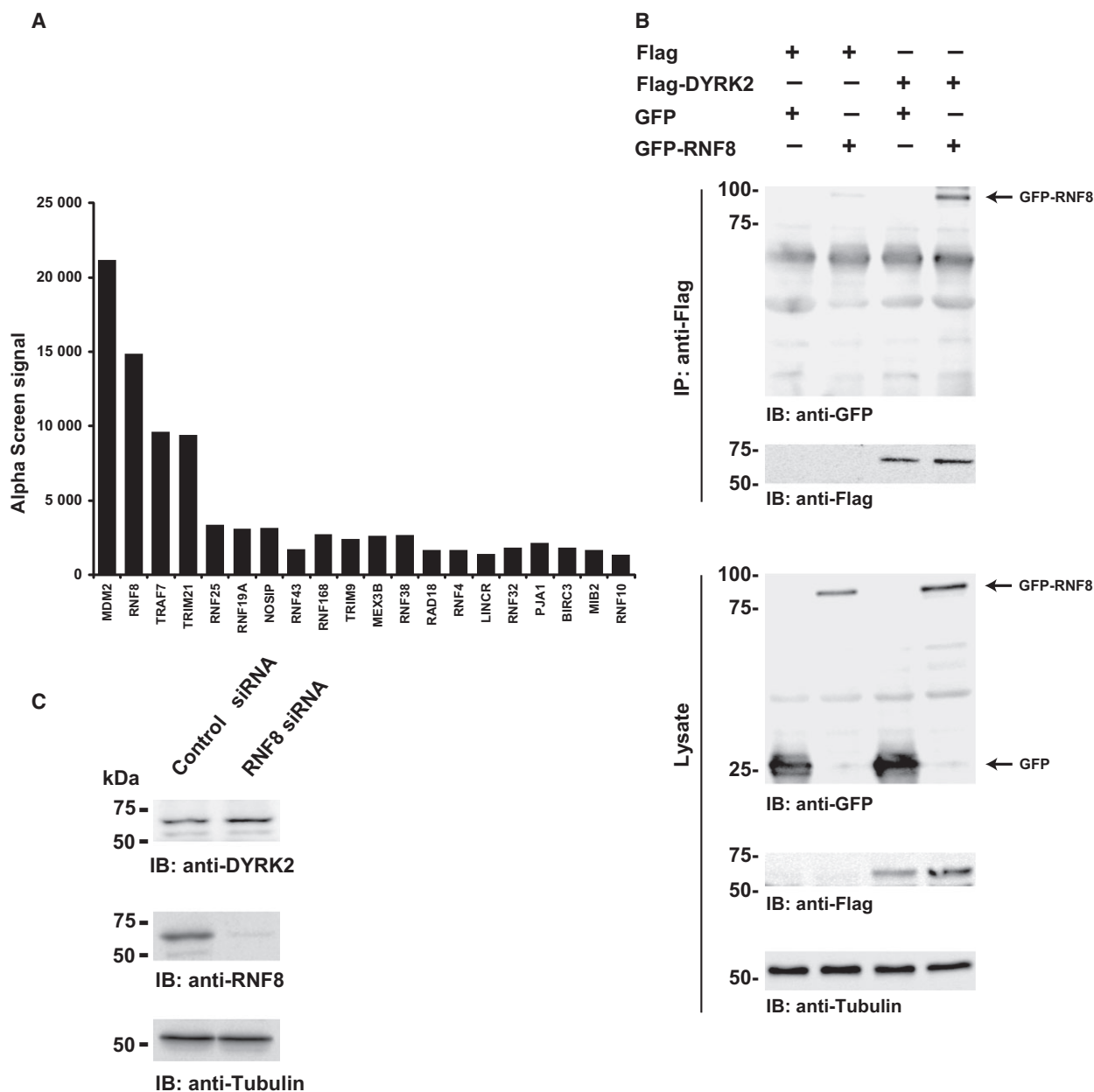


**Fig. 1.** RNF8 is a novel binding protein of DYRK2. (A) Screening results of E3 ubiquitin ligases binding to dual-specificity tyrosine phosphorylation-regulated kinase 2 (DYRK2) using the wheat germ cell-free expression system. (B) Human embryonic kidney (HEK) 293T cells were transfected with Flag-vector or Flag-DYRK2 and GFP-vector or GFP-RNF8. Lysates were immunoprecipitated with anti-Flag agarose and then subjected to immunoblotting. (C) Cells of the human osteosarcoma cell line U2OS were transfected with control siRNA or RNF8-specific siRNA. Lysates were analyzed by immunoblotting.

suggesting an essential role of DYRK2 in the monoubiquitination of γ-H2AX by RNF8 following genotoxic stress. Moreover, we quantified γ-H2AX monoubiquitination level in ADR-treated control and DYRK2 knockdown cells (Fig. S1B). To examine whether genotoxic stress was influenced by DYRK2 knockdown, we performed alkaline comet assay. The result indicated that the treatment with ADR in

DYRK2 knockdown cells increased the extent of percentage of damaged DNA in tail compared to control cells (Fig. S2). Given that DYRK2 is a Ser/Thr kinase, we examined the requirement of DYRK2 kinase activity in the monoubiquitination activity of RNF8 using the DYRK2 inhibitor, Harmine. An *in vitro* kinase assay was performed to evaluate the inhibition of DYRK2 activity by Harmine (Fig. S3). As shown
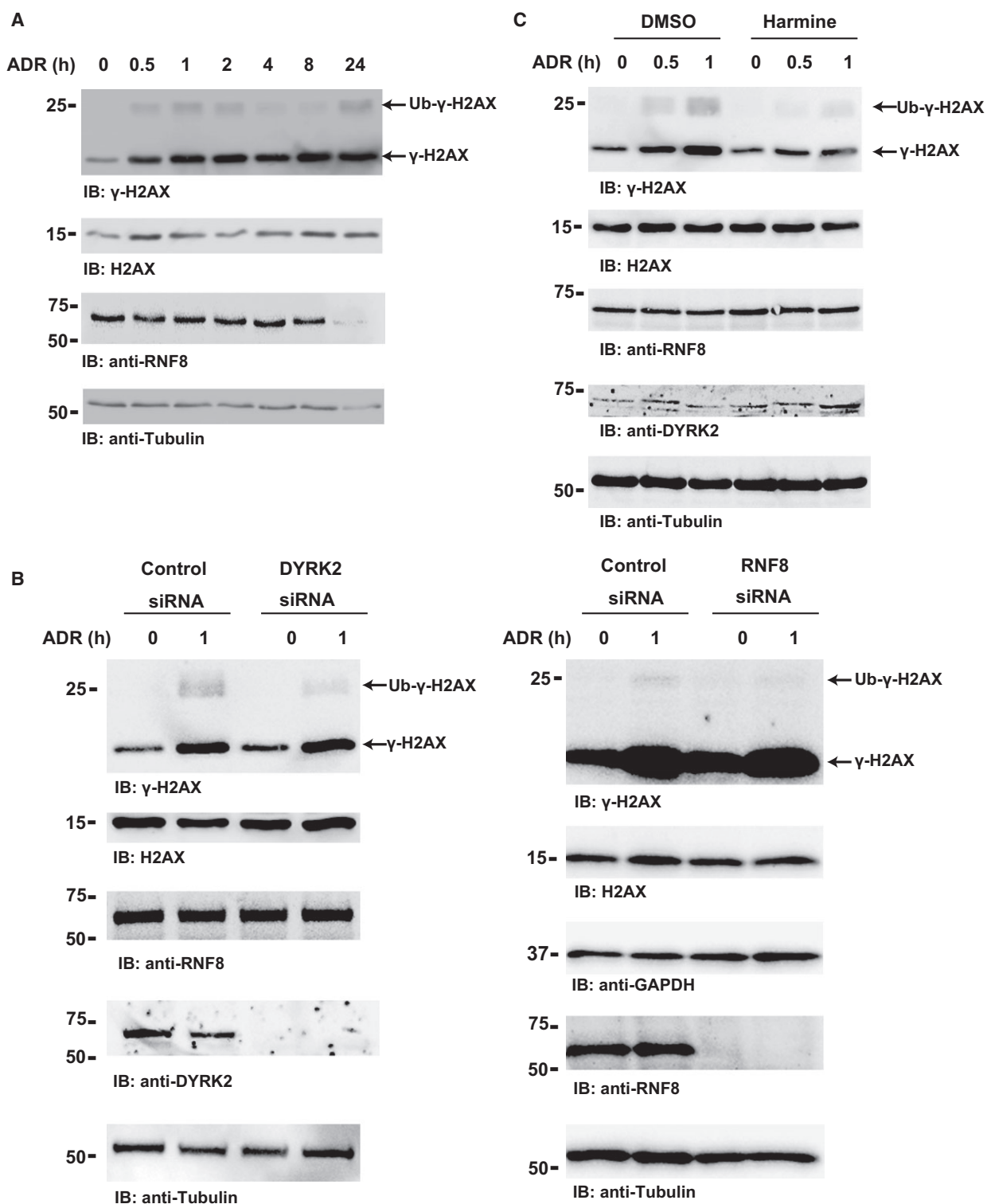
**Fig. 2.** DYRK2 is required for the monoubiquitination of γ-H2AX under genotoxic stress. (A) Cells of the human osteosarcoma cell line U2OS were treated with 2 μg·mL$^{-1}$ Adriamycin (ADR) for the indicated time points. Lysates were analyzed by immunoblotting. (B) U2OS cells were transfected with control siRNA or dual-specificity tyrosine phosphorylation-regulated kinase 2 (DYRK2) siRNA or RNF8 siRNA and then treated with ADR. Cell lysate was subjected to immunoblot analysis. (C) U2OS cells were treated with ADR in the presence or absence of Harmine. Cell lysates were isolated and analyzed by immunoblotting.
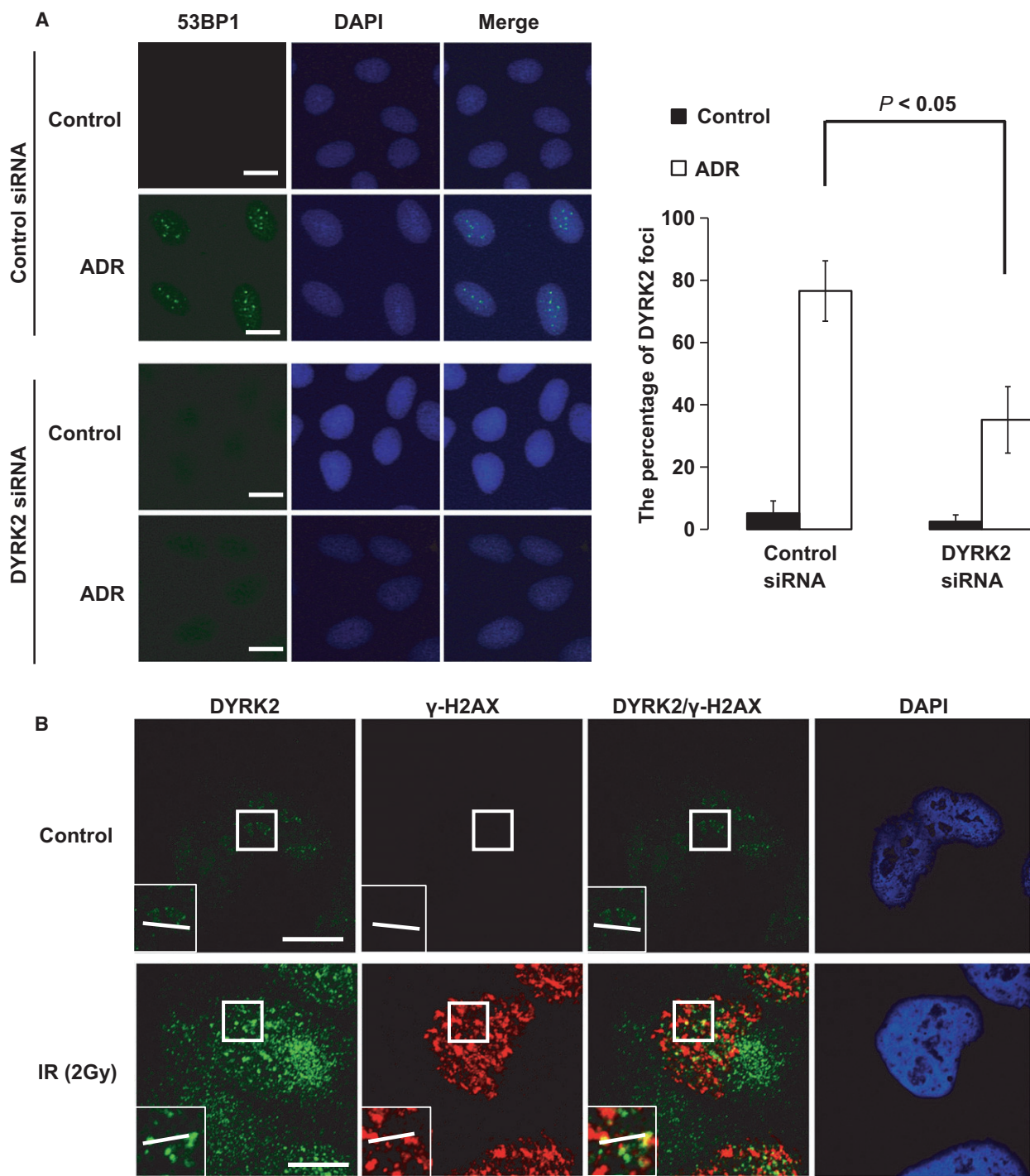
**Fig. 3.** DYRK2 contributes to 53BP1 foci formation under genotoxic stress, leading to DNA repair. (A) Cells of the human osteosarcoma cell line U2OS were transfected with control siRNA or dual-specificity tyrosine phosphorylation-regulated kinase 2 (DYRK2) siRNA and then treated with Adriamycin (ADR) for 4 h. Cells were stained with anti-53BP1. The nuclei were stained with DAPI. The quantification of cells with more than five 53BP1 foci was performed from three fields in two independent experiments. Statistical analysis was performed with the Student's t-test, and $P < 0.05$ was defined as statistically significant (mean $\pm$ SD; $n = 6$). Scale bar; 10 μm. (B) U2OS cells were treated with irradiation for 1 h. Cells were stained with anti-DYRK2 and anti-γ-H2AX. The nuclei were stained with DAPI. Scale bar; 10 μm.
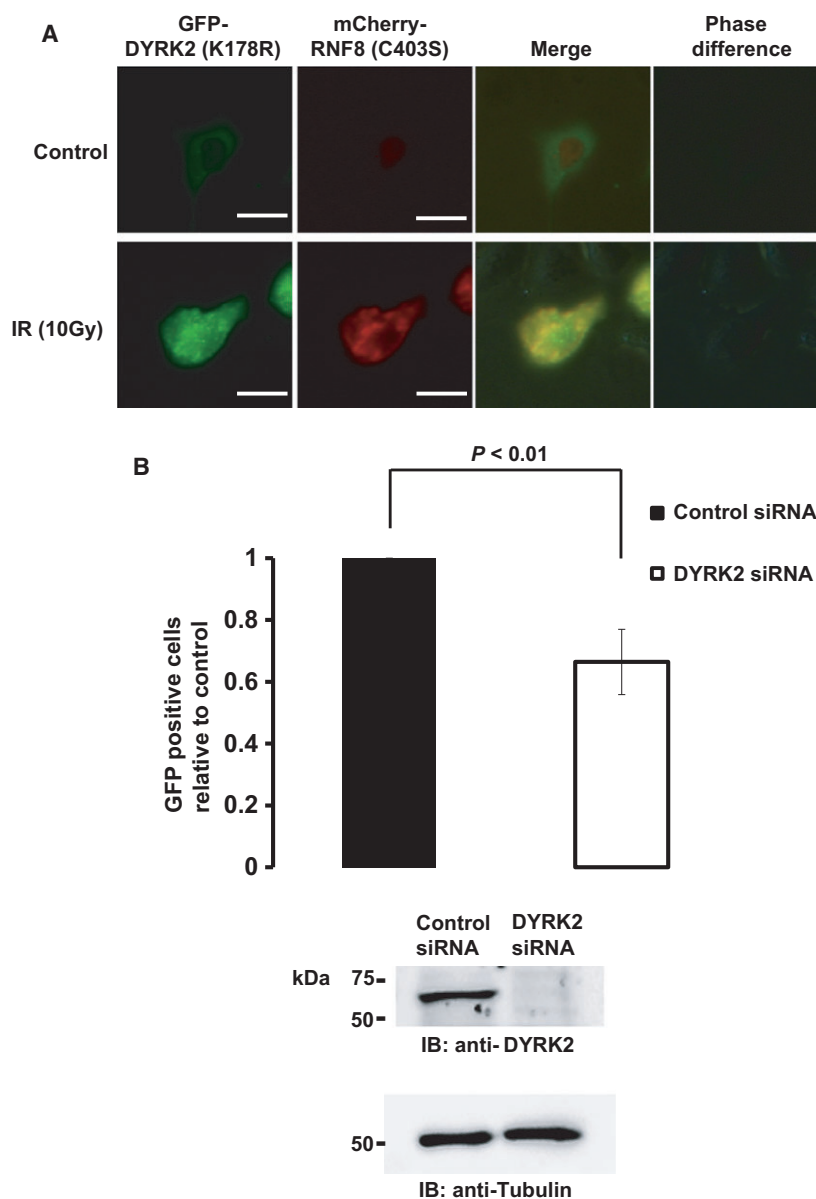
Fig. 4. DYRK2 and RNF8 are colocalized in the nucleus under genotoxic stress, leading to DNA repair. (A) U2OS cells were cotransfected with mCherry-tagged RNF8$^{C403S}$ mutant and GFP-tagged DYRK2$^{K178R}$ mutant and then treated with 10 Gy of irradiation. Scale bar; 10 μm. (B) The U2OS cell carrying the DR-GFP was transfected with control siRNA or DYRK2 siRNA, and then transfected with I-SceI plasmid. Statistical analysis was performed using the Student's t-test, and $P < 0.01$ was defined as statistically significant (mean ± SD; $n = 5$). The percentage of GFP-positive cells: control siRNA 2.54%, DYRK2 siRNA 1.40%.

previously [10], DYRK2 strongly phosphorylated p53 at Ser46. In contrast, Harmine effectively inhibited the p53 phosphorylation by DYRK2, confirming its inhibitory effect on DYRK2 (Fig. S3). In our previous study, we demonstrated the phosphorylation of p53 at Ser46 by DYRK2 in response to DNA damage [10]. To examine whether Harmine suppresses Ser46 phosphorylation in cells, U2OS cells were treated with ADR in the presence or absence of Harmine. DNA damage-induced Ser46 phosphorylation was attenuated by Harmine treatment (Fig. S3). To assess if Harmine inhibited damage-induced γ-H2AX monoubiquitination, U2OS cells were treated with Harmine, followed

by stimulation with ADR (Fig. 2C). DNA damage-induced γ-H2AX monoubiquitination was remarkably inhibited by Harmine treatment (Fig. 2C). These results indicated the requirement of DYRK2 kinase activity for the RNF8-mediated monoubiquitination of γ-H2AX.

## DYRK2 contributes to 53BP1 foci formation in response to genotoxic stress to induce DNA repair

The RNF8-mediated monoubiquitination of γ-H2AX triggers the recruitment of DNA repair molecules,
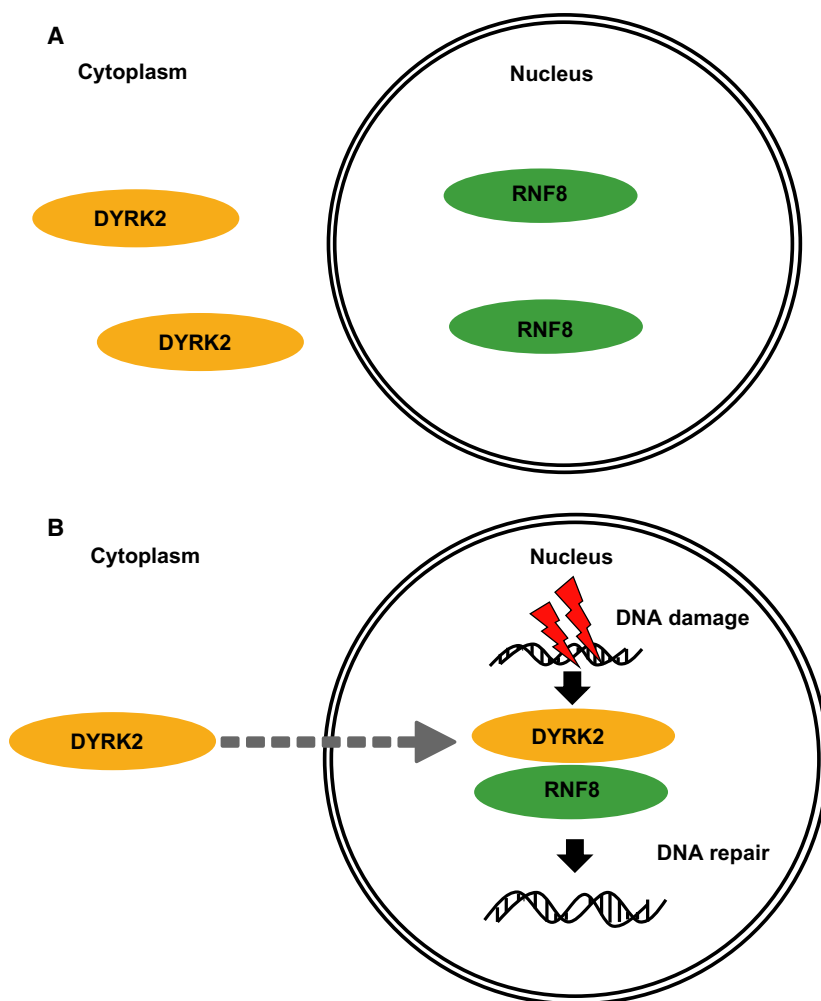
**Fig. 5.** The model for DNA repair mediated by DYRK2 and RNF8 in response to DNA damage. (A) Under unstressed condition, dual-specificity tyrosine phosphorylation-regulated kinase 2 (DYRK2) localizes in the cytoplasm, and RNF8 localizes in the nucleus. (B) Both DYRK2 and RNF8 were colocalized in the nucleus in response to DNA double-strand breaks (DSBs) in response to DNA damage.

including 53BP1, to the DNA damage sites. To verify the function of DYRK2 in DNA repair, we examined its requirement in the 53BP1 foci formation in response to genotoxic stress (Fig. 3A). 53BP1 formation, observed in ADR-treated U2OS cells, was markedly declined in DYRK2-depleted cells (Fig. 3A). To further investigate the function of DYRK2 on DNA repair, we examined the colocalization of endogenous DYRK2 and γ-H2AX under genotoxic stress. Interestingly, DYRK2 and γ-H2AX colocalized in the nucleus and exhibited foci-like distribution following DNA damage, suggesting their potential function at the DSB sites (Fig. 3B).

## DYRK2 and RNF8 are colocalized in the nucleus under genotoxic stress for DNA repair

To investigate the involvement of DYRK2 along with RNF8 in the repair of DSBs, mCherry-tagged

RNF8$^{C403S}$ mutant, and GFP-tagged DYRK2$^{K178R}$ mutant were colocalized in cells. RNF8$^{C403S}$ mutant, a catalytically inactive mutant was used [5] to avoid induction of excessive ubiquitination by overexpressing active RNF8 [27], and DYRK2$^{K178R}$, the kinase dead mutant was used to avoid induction of apoptosis by overexpressing active DYRK2 [10]. Under unstressed conditions, mCherry-tagged RNF8$^{C403S}$ mutant was localized in the nucleus, and GFP-tagged DYRK2$^{K178R}$ mutant was localized in the cytoplasm. Notably, both mCherry-tagged RNF8$^{C403S}$ mutant and GFP-tagged DYRK2$^{K178R}$ mutant were colocalized in the nucleus in response to DNA damage (Fig. 4A). These results suggest the cooperation of RNF8 with DYRK2 in the repair of DSBs. To examine this possibility, we performed an HR assay based on the I-SceI system [28]. Compared to control siRNA-transfected cells, depletion of DYRK2 failed to repair the DNA damage, which was triggered by

I-SceI (Fig. 4B). To determine if cell cycle distributions were influenced in these experimental settings, we performed cell cycle analysis. The result demonstrated that there was little if any difference between control and DYRK2 siRNA-transfected cells (Fig. S4). These findings strengthen the evidence indicating the involvement of DYRK2 in the regulation of DSB repair.

## Discussion

Post-translational modification, including phosphorylation and ubiquitination, initiates a quick response to DNA damage. Specifically, monoubiquitination of histone H2AX contributes to the recruitment of DNA repair factors at the DSBs. Besides histone ubiquitination, Fanconi anemia complementation group D2 (FANCD2) monoubiquitination promotes the assembly of FANCD2 and BRCA2/FANCD1 at DSB sites [29]. Furthermore, FANCI is ubiquitinated and evokes DNA repair along with FANCD2 [13]. These findings suggest that monoubiquitination promotes the assembly of checkpoint and repair factors at DSB sites. In the present study, we elucidated the involvement of DYRK2 in DNA repair at the DSB sites. We previously proved the activation of ATM within an hour in response to genotoxic stress and its subsequent attenuation suddenly at 4 h [25]. Corresponding to the activation of ATM, monoubiquitination of γ-H2AX by RNF8 was seen in the early stages of DNA damage (Fig. 2A), suggesting the dependence of RNF8 ubiquitination on ATM activation. Because ATM activates DYRK2 in response to DNA damage [25], the kinetics of ATM, DYRK2, and RNF8 activity possibly occurs simultaneously. In this study, we performed high-throughput screening based on wheat germ cell-free system and identified RNF8 as a binding partner for DYRK2 (Fig. 1A). RNF8 is well known for its role in DNA repair [30], however, its interaction with DYRK2 and their mechanism of action remains unknown. The present study demonstrates the interaction of DYRK2 and its colocalization with RNF8 under genotoxic-stressed conditions (Figs 1B and 4A), suggesting the cooperation between the two in repairing DSBs (Fig. 5A,B). In addition, the HR assay indicated reduced repair efficiency associated with the depletion of DYRK2 (Fig. 4B). Results from our previous studies have proved the involvement of DYRK2 in the induction of apoptosis and in the inhibition of EMT [9,10]. In this context, we identified a novel function of DYRK2 in the DNA repair pathway, aside from its tumor-suppressive functions. Considering that DYRK2 is a kinase,

it is expected to phosphorylate RNF8 in cells, whereas we could not detect DYRK2-mediated phosphorylation of RNF8. Further studies are required for clarifying the mechanism involved in the cooperation of DYRK2 and RNF8 in the DNA repair process for better understanding their role in cancer biology.

## Author contributions

TY, NTN, and KY were involved in the conception and design of the study. SY, KA, HT and TS contributed toward the development of methodology. TY, NTN, SY, KA, and HT contributed toward acquisition, analysis, and interpretation of data. TY, NTN, and KY contributed toward writing, reviewing, and/or revision of the manuscript. SY, KA, and HT provided technical or material support (i.e., reporting or organizing data, constructing databases). KY contributed toward study supervision.

## References

1 Bakkenist CJ and Kastan MB (2004) Initiating cellular stress responses. *Cell* **118**, 9–17.

2 Kinner A, Wu W, Staudt C and Iliakis G (2008) Gamma-H2AX in recognition and signaling of DNA double-strand breaks in the context of chromatin. *Nucleic Acids Res* **36**, 5678–5694.

3 Ma T, Keller JA and Yu X (2011) RNF8-dependent histone ubiquitination during DNA damage response and spermatogenesis. *Acta Biochim Biophys Sin (Shanghai)* **43**, 339–345.

4 Huen MS, Grant R, Manke I, Minn K, Yu X, Yaffe MB and Chen J (2007) RNF8 transduces the DNA-damage signal via histone ubiquitylation and checkpoint protein assembly. *Cell* **131**, 901–914.

5 Mailand N, Bekker-Jensen S, Faustrup H, Melander F, Bartek J, Lukas C and Lukas J (2007) RNF8 ubiquitylates histones at DNA double-strand breaks and promotes assembly of repair proteins. *Cell* **131**, 887–900.

6 Al-Hakim A, Escribano-Diaz C, Landry MC, O'Donnell L, Panier S, Szilard RK and Durocher D (2010) The ubiquitous role of ubiquitin in the DNA damage response. *DNA Repair (Amst)* **9**, 1229–1240.

7 Taira N, Mimoto R, Kurata M, Yamaguchi T, Kitagawa M, Miki Y and Yoshida K (2012) DYRK2 priming phosphorylation of c-Jun and c-Myc modulates cell cycle progression in human cancer cells. *J Clin Invest* **122**, 859–872.

8 Mimoto R, Taira N, Takahashi H, Yamaguchi T, Okabe M, Uchida K, Miki Y and Yoshida K (2013) DYRK2 controls the epithelial-mesenchymal transition in breast cancer by degrading Snail. *Cancer Lett* **339**, 214–225.

9 Yamaguchi N, Mimoto R, Yanaihara N, Imawari Y, Hirooka S, Okamoto A and Yoshida K (2015) DYRK2 regulates epithelial-mesenchymal-transition and chemosensitivity through Snail degradation in ovarian serous adenocarcinoma. *Tumour Biol* **36**, 5913–5923.

10 Taira N, Nihira K, Yamaguchi T, Miki Y and Yoshida K (2007) DYRK2 is targeted to the nucleus and controls p53 via Ser46 phosphorylation in the apoptotic response to DNA damage. *Mol Cell* **25**, 725–738.

11 Taira N and Yoshida K (2012) Post-translational modifications of p53 tumor suppressor: determinants of its functional targets. *Histol Histopathol* **27**, 437–443.

12 Taira N, Yamaguchi T, Kimura J, Lu ZG, Fukuda S, Higashiyama S, Ono M and Yoshida K (2014) Induction of amphiregulin by p53 promotes apoptosis via control of microRNA biogenesis in response to DNA damage. *Proc Natl Acad Sci USA* **111**, 717–722.

13 Smogorzewska A, Desetty R, Saito T, Schlabach M, Lach FP, Sowa ME, Clark AB, Kunkel TA, Harper JW, Colaiécovo MP *et al.* (2010) A genetic screen identifies FAN1, a Fanconi anemia-associated nuclease necessary for DNA interstrand crosslink repair. *Mol Cell* **39**, 36–47.

14 Takahashi H, Uematsu A, Yamanaka S, Imamura M, Nakajima T, Doi K, Yasuoka S, Takahashi C, Takeda H, Sawasaki T (2016) Establishment of a wheat cell-free synthesized protein array containing 250 human and mouse E3 ubiquitin ligases to identify novel interaction between E3 ligases and substrate proteins. *PLoS One* **11**, e0156718.

15 Takai K, Sawasaki T and Endo Y (2010) Practical cell-free protein synthesis system using purified wheat embryos. *Nat Protoc* **5**, 227–238.

16 Sawasaki T, Hasegawa Y, Tsuchimochi M, Kamura N, Ogasawara T, Kuroita T and Endo Y (2002) A bilayer cell-free protein synthesis system for high-throughput screening of gene products. *FEBS Lett* **514**, 102–105.

17 Strausberg RL, Feingold EA, Grouse LH, Derge JG, Klausner RD, Collins FS, Wagner L, Shenmen CM, Schuler GD, Altschul SF *et al.* (2002) Generation and initial analysis of more than 15,000 full-length human and mouse cDNA sequences. *Proc Natl Acad Sci USA* **99**, 16899–16903.

18 Ajioka I, Maeda T and Nakajima K (2006) Large-scale correlation of DNA accession numbers to the cDNAs in the FANTOM full-length mouse cDNA clone set. *Keio J Med* **55**, 107–110.

19 Sawasaki T, Kamura N, Matsunaga S, Saeki M, Tsuchimochi M, Morishita R and Endo Y (2008) Arabidopsis HY5 protein functions as a DNA-binding tag for purification and functional immobilization of proteins on agarose/DNA microplate. *FEBS Lett* **582**, 221–228.

20 Gyori BM, Venkatachalam G, Thiagarajan PS, Hsu D and Clement MV (2014) OpenComet: An automated tool for comet assay image analysis. *Redox Biol* **2**, 457–465.

21 Singh NP, McCoy MT, Tice RR and Schneider EL (1988) A simple technique for quantitation of low levels of DNA damage in individual cells. *Exp Cell Res* **175**, 184–191.

22 Nihira NT and Yoshida K (2015) Engagement of DYRK2 in proper control for cell division. *Cell Cycle* **14**, 802–807.

23 Maddika S and Chen J (2009) Protein kinase DYRK2 is a scaffold that facilitates assembly of an E3 ligase. *Nat Cell Biol* **11**, 409–419.

24 Jung HY, Wang X, Jun S and Park JI (2013) Dyrk2-associated EDD-DDB1-VprBP E3 ligase inhibits telomerase by TERT degradation. *J Biol Chem* **288**, 7252–7262.

25 Taira N, Yamamoto H, Yamaguchi T, Miki Y and Yoshida K (2010) ATM augments nuclear stabilization of DYRK2 by inhibiting MDM2 in the apoptotic response to DNA damage. *J Biol Chem* **285**, 4909–4919.

26 Kolas NK, Chapman JR, Nakada S, Ylanko J, Chahwan R, Sweeney FD, Panier S, Mendez M, Wildenhain J, Thomson TM *et al.* (2007) Orchestration of the DNA-damage response by the RNF8 ubiquitin ligase. *Science* **318**, 1637–1640.

27 Kato K, Nakajima K, Ui A, Muto-Terao Y, Ogiwara H and Nakada S (2014) Fine-tuning of DNA damage-dependent ubiquitination by OTUB2 supports the DNA repair pathway choice. *Mol Cell* **53**, 617–630.

28 Nakada S, Yonamine RM and Matsuo K (2012) RNF8 regulates assembly of RAD51 at DNA double-strand breaks in the absence of BRCA1 and 53BP1. *Cancer Res* **72**, 4974–4983.

29 Wang X, Andreassen PR and D'Andrea AD (2004) Functional interaction of monoubiquitinated FANCD2 and BRCA2/FANCD1 in chromatin. *Mol Cell Biol* **24**, 5850–5862.

30 Kobayashi S, Kasaishi Y, Nakada S, Takagi T, Era S, Motegi A, Chiu RK, Takeda S and Hirota K (2015) Rad18 and Rnf8 facilitate homologous recombination by two distinct mechanisms, promoting Rad51 focus formation and suppressing the toxic effect of nonhomologous end joining. *Oncogene* **34**, 4403–4411.

## Supporting information

Additional Supporting Information may be found online in the supporting information tab for this article:

**Fig. S1.** Knockdown of DYRK2 attenuated γ-H2AX monoubiquitination level.

**Fig. S2.** Doxorubicin genotoxic stress was influenced by DYRK2 knockdown.

**Fig. S3.** Harmine inhibited DYRK2 kinase activity.

**Fig. S4.** Cell cycle distributions in control and DYRK2 siRNA-transfected cells.